Int J Adv Manuf Technol
DOI 10.1007/s00170-016-8490-y

ORIGINAL ARTICLE

# Experimental study of lateral pass width in conventional and vibrations-assisted ball burnishing

**G. Gomez–Gras[1] · J. A. Travieso–Rodriguez[1] · R. Jerez–Mesa[1] · J. Lluma-Fuentes[2] · B. Gomis de la Calle[1]**

Received: 22 June 2015 / Accepted: 4 February 2016


**Abstract** Burnishing is a mechanical finishing operation performed on workpieces to enhance their surface quality through plastic deformation. One of the main issues to understand the overall process is the behavior of the elastoplastic deformations caused by the burnishing ball on the workpiece. The first burnishing passes performed on the workpiece surface lead to its plastic strain and self-hardening, thus influencing the results of consecutive passes. Some references have studied the phenomenon of indentation, finding that there is a certain self-hardening coefficient threshold which allows to predict the presence of pile-ups at the edges of the indentation path. Nevertheless, burnishing is not a single-pass operation. On the contrary, burnishing a whole surface requires successive adjacent and/or overlapping passes, i.e., parallel passes separated consecutively a certain lateral pass width. No reference has been found in the literature defining the adequate values of the lateral pass width with regards to the pile-up effect to enhance the final topology of the burnished surface. This paper explores that influence by studying the presence of the pile-up effect after burnishing a single or several overlapping passes on two materials (aluminum and steel), by characterizing the topology of the generated path. Afterwards, two adjacent passes are performed, varying the lateral pass width, to compare the final surface roughness derived from each operation. An optimum value for the lateral pass width was found, to improve the final roughness after burnishing in different conditions and to increase the productivity of the process.

**Keywords** Ball burnishing · Lateral pass width · Pile up · Steel · Aluminum · Indentations

## 1 Introduction

Burnishing is a mechanical and chipless finishing operation, performed on workpieces to enhance their surface quality, and improve their performance to highly demanding working regimes [1–4]. Unlike other finishing processes, such as grinding, lapping, polishing, or honing which have similar results in terms of surface roughness, ball burnishing is especially beneficial in terms of induced compressive residual stresses that improve fatigue performance of treated parts [5–7]. These effects are especially noticeable in parts subjected to fatigue life wear and friction have also proved to be enhanced [8]. This is especially interesting in todays industry, for mechanical parts must comply with rapidly increasing mechanical demands and competitiveness. Several applications have also been found enhancing the quality of injection molds [9].

The ball burnishing process is performed with a burnishing tool, such as the one from Travieso-Rodriguez et al. [10] attached to the tool-holder or spindle of conventional machine tools or CNC machines. In all cases, the principle of action is the same: a calibrated and controlled force

✉ R. Jerez–Mesa
ramon.jerez@upc.edu

G. Gomez–Gras
giovanni.gomez@upc.edu

[1] Mechanical Engineering Department, Universitat Politècnica de Catalunya, C. Comte d'Urgell, 187 Barcelona, Spain

[2] Materials Science and Metallurgical Engineering Department, Universitat Politècnica de Catalunya, C. Comte d'Urgell, 187 Barcelona, Spain

Published online: 20 February 2016

is applied to the workpiece through a sphere capable of rolling freely, supported by a bearing in the tip tool. The ball glides over the objective surface in several successive passes, deforming the peaks of the roughness profile, thus filling in the valleys with their material [11].

The results of a burnishing operation are highly dependent on the initial surface conditions [12], although that is not the only influencing factor. This paper deals with the interaction mechanisms between the burnishing ball and the treated material. The constant action of the burnishing ball through controlled pressure causes elastoplastic strains on the surface, leading to its self-hardening. These elastoplastic deformations make the analysis of the process more difficult in terms of understanding how the tool and the material interact [13].

One of the aspects defining the final topology of a burnished surface is the remarkable flow of material towards the edges of the imprinted path, thus generating what is known as pile-ups and sink-ins. The transverse shape of the imprint is mainly defined by its depth ($p_h$), width ($a_h$), and pile-up height ($h_a$) (Fig. 1). Its presence depends on several factors described below, and its existence is an important factor to bear in mind when defining the burnishing strategy of a certain workpiece because of its influence on the finishing of its surface, as acknowledged in Lopez de la Calle et al. [14]. That is to say, burnishing a surface consists on executing several adjacent passes which are influenced by the pile-ups resulting from the immediately previous ones. Despite of that fact, the lateral pass between adjacent passes has not been studied as a relevant variable in the process.

The formation of either pile-ups or sink-ins is directly related to the cold-hardening (or strain-hardening) characteristics of the material. Some authors such as Gao [15] and Gao et al. [16] have studied the influence of the strain-hardening properties of a certain material on its behavior towards burnishing. Sequera et al. [17] concluded that strain hardening of an INCONEL 718 specimens was dissimilar in the parallel or orthogonal direction of the burnishing passes, mainly due to the increase of the burnishing track depth. Qu et al. [18] confirmed their experimental results by developing a FEA model, thus supporting the idea that pile-up formation depends on the indented material. That is, the pile-up phenomenon is not common to all materials. In their analysis Nix and Gao [19] introduced different indenter geometries, confirming that it is a relevant factor in the process and defining the magnitude of the pile-ups and its hardness profile depending on the indenter geometry.

The fact that the material and shape of the indenter influence the final burnished surface has led some researchers to find a way to predict the behavior of materials when burnished through the definition of the self-hardening coefficient ($n$). Based on its calculation, a material is expected to present pile-ups after burnishing when $n > 0.25$ and sink-ins when $n < 0.25$ [20]. This coefficient can be related to the $c^2$ ratio, which represents the relationship between the depth of the contact of the indenter with the burnished surface and its penetration depth. In the case of spherical indentation (i.e., ball burnishing), the pile-up effect would occur when $c^2 > 1$.

In this paper, a ball-burnishing tool has been used to perform the tests. This tool is able to work under two conditions, that is, conventional burnishing (i.e., non-vibration-assisted), and another assisted by a 2.5 kHz vibration. The latter has proved to perform better final results in terms of surface roughness, as shown in the same reference.

To analyze the topography of the burnishing imprint, the processing parameters selected for the operation must be considered. These parameters are:

1. Lateral pass width, $b$: the distance between two successive adjacent burnishing passes.
2. Number of overlapping burnishing passes, $N$: number of repetitions of burnishing passes following the same path (no lateral pass width taken between each of them).
3. Applied force, $F$: calibrated and executed by the burnishing tool.
4. Type of burnishing, that is, non-vibration-assisted ball burnishing (NVABB) and vibration-assisted ball burnishing (VABB).

The aim of this paper is analyzing the topography generated by a burnishing tool developed by Gomez-Gras et al. [21], using different technological parameters on two different materials. This experimental study is framed within a series of research activities to characterize the used burnishing tool, currently in a definition stage for its industrial

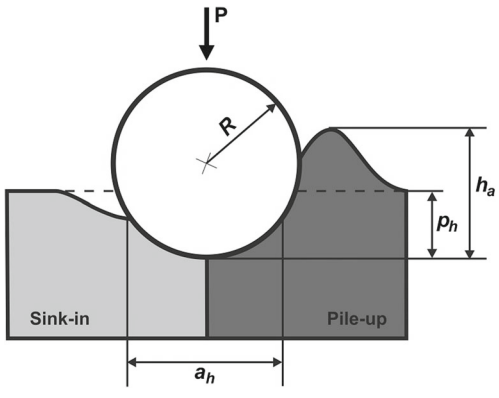


**Fig. 1** Diagram of the contact amongst a burnishing ball and a workpiece. The characteristic parameters of the indented profile are defined as $a_h$ imprint width; $p_h$ imprint depth; $h_a$ pile-up height; $R$ burnishing-ball radius; and $P$ burnishing force

application. Hence, the industrial interest of the results shown in this paper.

## 2 Materials and methods

Two materials were used for the specimens of this experimental research: aluminum 2017 and steel AISI 1038. These two materials were selected because of their industrial relevance in the first place, as well as for their different behaviors towards the pile-up phenomena (i.e., different strain-hardening coefficients).

Burnishing results are dependent on their processing parameters, but also on the workpiece initial conditions [22]. Burnished surfaces of the specimens of both materials were therefore pre-processed with a face-milling operation to ensure that their initial average surface roughness was the same. In the aluminum specimen, the average roughness was $R_a = 1.591\ \mu$m, while in the steel specimen, it was $R_a = 2.239\ \mu$m. Afterwards, the burnishing tool was attached to a CNC LAGUN MC600 milling machine. The specimens were then treated with a NVABB and a VABB processes. The tool itself, working with a 10-mm ball, was the same for both processes and had 600 mm/min feed for all operations. Connecting it to a vibrations generator or not allows to switch from one burnishing regime to the other.

The experiments were developed in two phases. The first one aims to characterize the topography of the imprints of several ball-burnishing operations, using different forces and number of overlapping passes. The second stage starts from the measurement of topological parameters resulting from the first phase and consists of executing two consecutive ball burnishing passes separated by a certain lateral pass width.

### 2.1 First phase: characterization of burnishing imprint

Four specimens were burnished in this phase, two of them (one of each material) treated with a NVABB process and the other two with a VABB one. Twelve indentations were performed on each specimen, varying the number of passes and applied force (Fig. 2). The testing levels for each of these parameters were selected according to previous studies [23, 24].

Every imprint resulting from each burnishing operation was measured 20 times with a Mitutoyo SURFPAK-SJ V3 profilometer, using a 2.5-mm cut-off length. The signals were processed to obtain an average characteristic profile (i.e., measuring its width, depth, and pile-up height, if applicable). That average profile would represent each processing condition for their subsequent comparison.

### 2.2 Second phase: recommended lateral pass width

Two specimens of steel and aluminum are used in this case. The lowest force and highest number of passes used in the first stage were discarded because they showed no significantly different results in the first phase of operations. Figure 3 shows the levels of the process parameters in both tested specimens.

In this phase, after each first burnishing operation, a second pass was performed both of them separated by a length called lateral pass width, $b$, as indicated in Fig. 4. In order to define the testing interval, several tests were previously performed varying the lateral pass width. Although for both materials, the lowest value for average surface roughness was obtained when $b = l$ (see Fig. 5), a plateau was observed between $b = l/2$ and $b = l$. This fact justifies the selection of the two extremes of the plateau for testing. The first one, $l$, is the distance between the deepest valley and highest peak observed in the imprint analysis of the first phase. The second tested value for $b$ has been half that distance, $l_m = l/2$.

This second testing phase results in 480 new signals, representing the shape of the imprints that derives from two subsequent burnishing passes. The signals show the evolution of both extremes of the plateau and allow for suggesting operation conditions in each studied case.

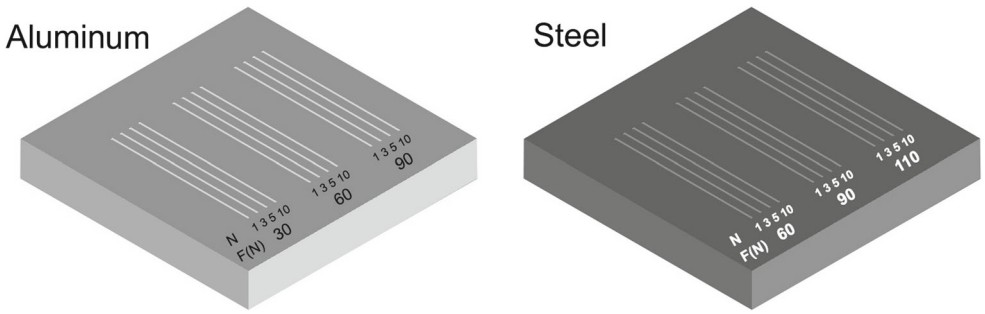


**Fig. 2** Specimens for the first experimental phase and levels of each burnishing variable. Dimensions 100 × 70 × 20 mm. *Left* 2017 aluminum and *right* AISI 1038

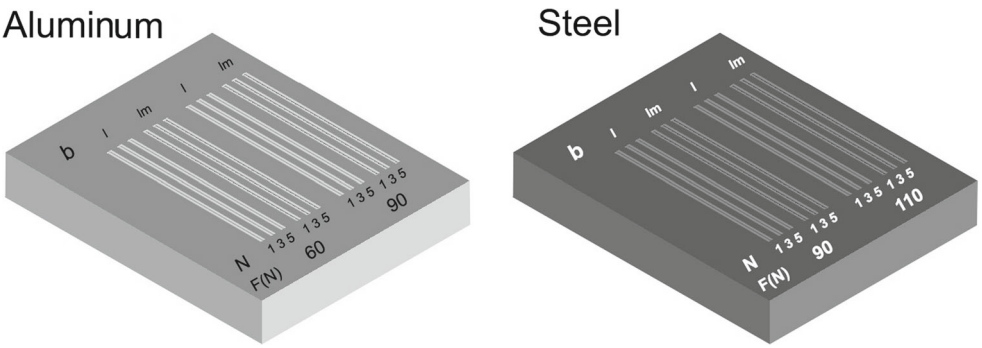


**Fig. 3** Specimens for the second experimental phase and levels of each burnishing variable. Dimensions 100 × 70 × 20 mm. *Left* indicates the 2017 aluminum and *right* indicates the AISI 1038

## 3 Results and discussion

### 3.1 First phase

#### *3.1.1 Aluminum 2017*

The results for every group of testing conditions have been represented in Figs. 6 and 7, for NVABB and VABB processes, respectively. The different force values used to test aluminum specimens define the width and depth of the imprint, thus influencing the magnitude of the pile-up as well. This fact confirms the statements presented at the beginning of this paper. As the number of passes increase, so does strain, and that has an impact on the final topology of the imprint. For all analyzed parameters, the most significant changes are for imprints with 1, 3, and 5 overlapping burnishing passes, being less noticeable for those with 10. This trend is more significant for low burnishing forces, that is, the difference of width, depth, and pile-up height measurements between 5 and 10 overlapping burnishing passes is higher for 30 N tests than for 90 N, due to the faster saturation of the material hardening.

Of special interest is the accomplished pile-up height. For a 30 N burnishing force, the rise in strain is 58 % from 1 to 3 overlapping burnishing passes, 49 % from 3 to 5 overlapping burnishing passes, and 11 % from 5 to 10 overlapping burnishing passes. On the other hand, for a 90 N force, increments are 20, 25, and 10 %, respectively. This lack of homogeneity in strain increase means that the burnishing force is not the only relevant element in the overall process.

A more thorough inspection of the imprints width evidences a better performance of the VABB process. This fact can be explained by the higher energy, that the vibrations induce into the system, which generates higher plastic deformation in the surface of the material, as explained by Travieso-Rodriguez et al. [25]. These results are yet very moderate in relative terms: 6.7 and 8 % when changing from 30 to 60 N, and 60 to 90 N, respectively. No relevant changes have been detected that can be attributed to the number of passes.

#### *3.1.2 AISI 1038 steel*

Figure 8a, b shows the results for the steel specimens. The main difference with respect to the results in the aluminum specimens is that pile-up phenomena is missing,

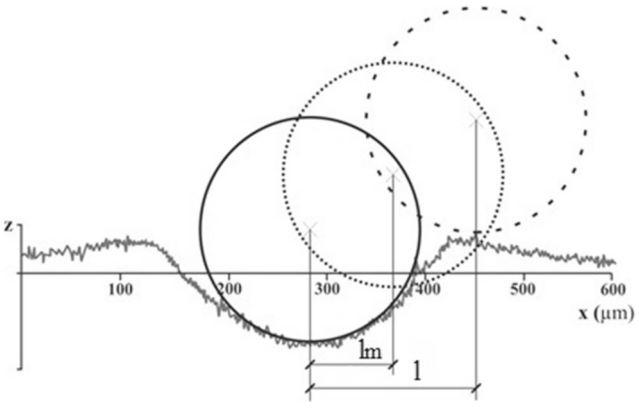


**Fig. 4** Diagram of lateral pass width (**b**) used in the experiments, represented on a real profile obtained in the first phase of experimentation

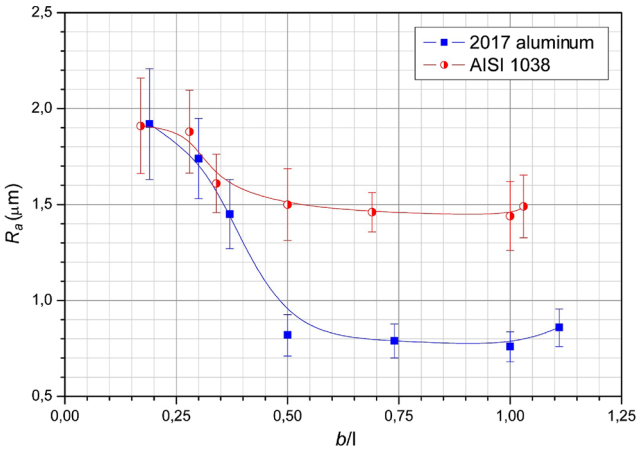


**Fig. 5** Average roughness for specimens treated with a NVABB process, $F = 90$ N and $N = 1$

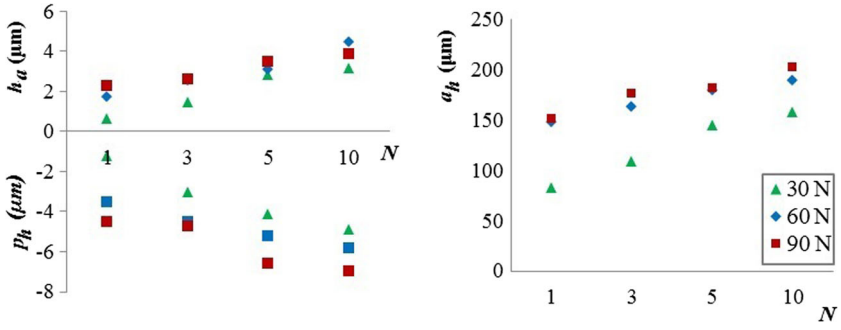


**Fig. 6** Evolution of imprint dimensions depending on number of passes ($N$) and applied force ($F$) for the NVABB specimens

as explained above. Besides this consideration, results in steel specimens are very similar to the ones obtained in aluminum. The strain magnitude is directly proportional to the applied force. Most significant changes occur between 3 and 5 overlapping burnishing passes. Burnishing with 10 overlapping passes does not show any considerable increment in deformation.

The imprint widths for VABB specimens show similar results when executed with 90 and 110 N (Fig. 8b). This behavior may be due to strain-hardening being too high for these force levels, and the burnishing system would eventually require higher forces to cause significant plastic deformations. In addition, the frequency of the vibrations that assist the process may not be sufficient to induce enough energy into the system, and therefore, caused deformations cannot be higher [26].

By all means, the effect of assisting the burnishing process with vibrations has satisfactory results. For instance, the imprint depth increased by 46 % when raising the burnishing force from 60 to 90 N, both in the NVABB and VABB processes. From 90 to 100 N, the increase was 57 % in the NVABB process and 24 % in the VABB.

The influence of vibrations on the plastic deformation of steel specimens shows a similar trend. The imprint increases as force does and that very same increment is higher when the process is assisted by vibrations. That is more noticeable in the imprint width value, which changed from 40 to 50 % when assisted by vibrations.

The results explained above have characterized the imprint topography in several testing conditions and originate the data needed to analyze the shape of the burnishing imprint when burnished with two adjacent passes.

### 3.2 Second phase

The distance between the imprint deeper point and the highest point of the profile (l), measured on the imprints performed during the first phase of the experiment, has been considered as an input parameter to tackle the second phase (Table 1). In the case of aluminum specimens, the highest point of the profile coincides with the highest pile-up point.

For this group of tests, burnishing parameters were slightly changed, and two adjacent burnishing passes were performed taking two different lateral passes (both extremes of the roughness plateau). In the first scenario, the lateral pass was l, that is, the center of the burnishing sphere was made coincident with the highest point caused by the first burnishing (lateral pass width = l). In the second case, lateral width was half that distance ($l_m$).

Figure 9 illustrates the comparison between the burnishing imprint section after one pass, and the results of burnishing with two consecutive paths taking a lateral pass width of l and $l_m$. Figure 9a refers to aluminum specimens indented with the process assisted by vibrations applying 90 N. The shape corresponding to one pass (black signal) is more regular as the other two, in which the profile is clearly

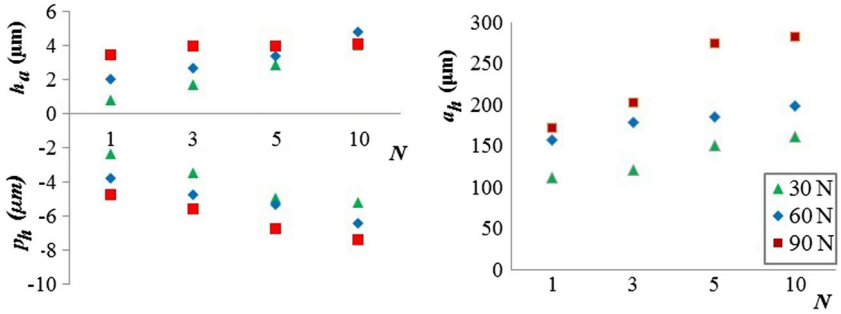


**Fig. 7** Evolution of imprint dimensions depending on number of passes ($N$) and applied force ($F$) for the VABB specimens

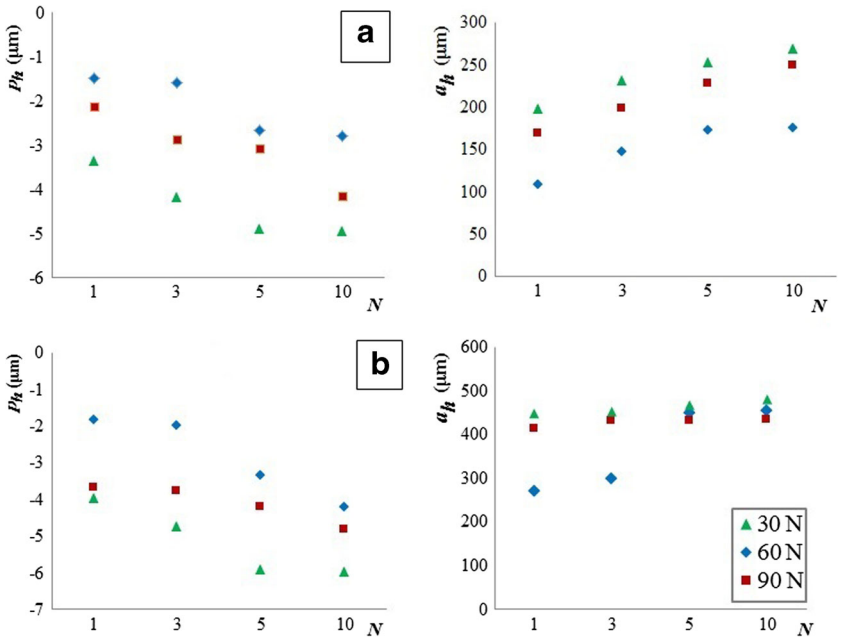


**Fig. 8** Evolution of imprint dimensions depending on number of passes ($N$) and applied force ($F$). **a** NVABB specimens and **b** VABB specimens

affected by the second pass. In all cases, pile-ups are noticeable, as the material has flown towards the flanks of the burnishing path due to strain-hardening.

The redistribution of the material due to the second pass is evident when it is performed on the very peak of the previous pile-up (that is, $b = \mathrm{l}$, blue signal at Fig. 9a). At both sides of the newly generated profile, the displacement of material after strain hardening is visible. The new pile-ups reach in any case lower heights with regards to the ones obtained with the single-pass burnishing. As for the second tested lateral pass, $b = l_m$, the effects of the second pass on the previous imprint are also conspicuous, although at first sight it seems that the carrying surface is planer when the lateral pass $b = \mathrm{l}$ is used.

The same phenomena has been proved on the tested steel specimens. The signals corresponding to the three different

**Table 1** Values of lateral pass width, $b$, for each testing condition of both materials

| | l (mm) | | |
|---|---|---|---|
| | 1 single pass | 3 overlapping passes | 5 overlapping passes |
| Al2017 NVABB | | | |
| 60 N | 0.250 | 0.270 | 0.280 |
| 90 N | 0.270 | 0.280 | 0.290 |
| Al2017 VABB | | | |
| 60 N | 0.280 | 0.290 | 0.310 |
| 90 N | 0.300 | 0.320 | 0.330 |
| AISI 1038 NVABB | | | |
| 90 N | 0.290 | 0.320 | 0.350 |
| 110 N | 0.320 | 0.330 | 0.360 |
| AISI 1038 VABB | | | |
| 90 N | 0.320 | 0.360 | 0.370 |
| 110 N | 0.350 | 0.370 | 0.390 |

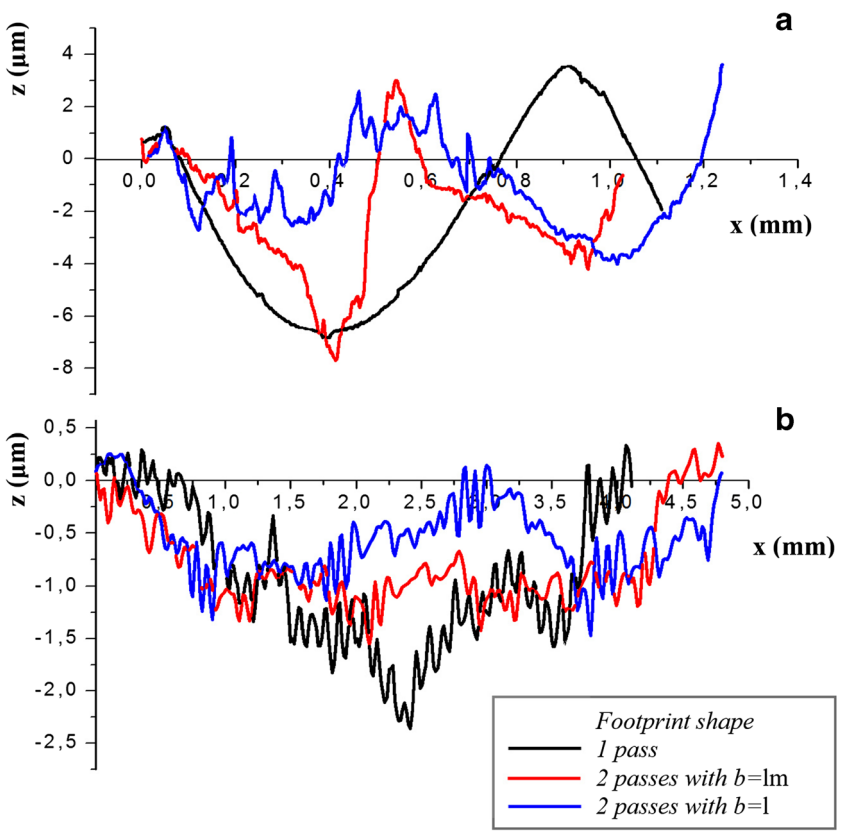


**Fig. 9** Comparison of burnishing imprints for three conditions of the VABB process: simple burnishing, two adjacent passes taking $b = \mathrm{l}$, and two adjacent passes taking $b = l_m$. **a** Aluminum 2017 specimens subjected to 90 N and **b** AISI 1038 steel specimens subjected to 110 N

testing conditions have been compared at Fig. 9b, for 110 N applied in a vibrations-assisted process. The influence of the second pass on the imprint profile is not so visible as in the case of aluminium, because of the lack of pile-up effect in this material. Nevertheless, the overall behavior is comparable to that of aluminum. As the ball burnishes at a second pass taking a lateral offset of $b = \mathrm{l}$ (blue signal), the profile slightly changes of distribution. The case of $b = l_m$ is similar. This means that, for steel materials, the optimal values for the lateral pass width should be decided in terms

**Table 2** $R_a$ ($\mu$m) measured for aluminum and steel specimens in all testing conditions and for both lateral pass widths considered

| | 2017 aluminum | | | | AISI 1038 steel | | | |
|---|---|---|---|---|---|---|---|---|
| $F$ (N) | 60 | | 90 | | 90 | | 110 | |
| $b$ (mm) | $l$ | $l_m$ | $l$ | $l_m$ | $l$ | $l_m$ | $l$ | $l_m$ |
| $N$ | | | | | | | | |
| | NVABB | | | | NVABB | | | |
| 1 | 0.9194 | 1.0142 | 0.7533 | 0.8173 | 1.4291 | 1.4902 | 0.7205 | 0.9882 |
| 3 | 0.9068 | 1.0010 | 0.5787 | 0.7086 | 1.2102 | 1.3543 | 0.7548 | 0.9956 |
| 5 | 0.8572 | 0.9865 | 0.5217 | 0.6578 | 1.1134 | 1.3480 | 0.7087 | 0.8272 |
| | VABB | | | | VABB | | | |
| 1 | 0.7574 | 0.9495 | 0.6478 | 0.6943 | 1.1208 | 1.2706 | 0.5984 | 0.6256 |
| 3 | 0.6824 | 0.8209 | 0.5784 | 0.6298 | 1.0001 | 1.1943 | 0.5883 | 0.6082 |
| 5 | 0.5901 | 0.7628 | 0.3983 | 0.6568 | 0.8284 | 0.8493 | 0.5493 | 0.5813 |

**Table 3** Recommended values of lateral pass width, $b$, for both tested ball burnishing processes and both materials

| | | |
|---|---|---|
| 2017 aluminum | NVABB | $b = 0.29$ mm ($F = 90$ N) |
| | VABB | $b = 0.33$ mm ($F = 90$ N) |
| AISI 1038 steel | NVABB | $b = 0.36$ mm ($F = 110$ N) |
| | VABB | $b = 0.39$ mm ($F = 110$ N) |

of productivity, as pile-up does not occur. Therefore, it is advisable to apply the condition $b = l$ for the lateral pas width, in order to reduce processing times.

Finally, the average surface roughness has been introduced into the discussion about the optimum lateral pass width for ball burnishing in order to support the analysis of how final surface profile of workpieces is configured when changing the lateral pass width. To that effect, the average surface roughness, $R_a$, has been calculated for each of the performed experiments (Table 2) so that a relation can be established between surface quality and lateral pass width. The maximum error found for these values is 7.9 %.

Results of average surface roughness confirm the appreciations derived from the superposition of signals as presented in Fig. 9. Both materials show better results if the second burnishing path is performed by taking a lateral pass width of l. The improvement in roughness is limited but together with the productivity criterion is enough to justify taking l as lateral pass width.

On the other hand, the relationship between the burnishing force and the final average roughness is, as expected, inversely proportional. Best results are also obtained in all cases by performing five overlapping burnishing passes.

The most relevant differences in average surface roughness are caused by the introduction of vibrations in the process as a means of assistance. Average roughness obtained with one pass of the VABB process is very similar, or even better, than that resulting from a conventional NVABB one. The relevance of this finding lays in the fact that productivity can be improved with the VABB process.

Technical recommendations for both processes (assisted and non-vibration-assisted) have been deduced from the experimental tests explained in this paper. Optimal values of lateral pass width, in terms of surface roughness, have been defined for each combination of technological group of parameters (Table 3).

## 4 Conclusions

In this paper, the topological characteristics of burnishing imprints on aluminum 2017 and AISI 1038 steel have been studied after different combinations of burnishing parameters, considering both the conventional process and the vibrations-assisted one. The measured results of that first geometrical stage were the input to a second phase, in which the best value for the lateral pass width between adjacent burnishing passes was studied, in terms of surface roughness. The following conclusions can be extracted

1. A different self–hardening behavior in aluminum 2017 and steel AISI 1038 can be observed and confirmed experimentally, thus affecting differently the burnishing strategy for both materials. The aluminum 2017 shows prominent pile-ups at the limits of the burnished paths, whereas the steel does not show this effect.
2. An experimental relationship between the geometry of a burnishing imprint and the applied burnishing parameters can be established. Specifically, for a ratio $0.5 < b/l < 1$, that is, the relation between the lateral pass width between adjacent burnishing paths and the length between a pile-up peak and the bottom of the burnishing imprint, no significant influence of the lateral pass width is observed on the final average roughness, given a combination of force and number of passes for a certain material.
3. The value of the recommended lateral pass width is a technological parameter which depends mainly on the material and the level of applied force.
4. There is a remarkable influence of the vibrations on the optimal value of lateral pass width observed. The process assisted by vibrations requires wider values of lateral pass width, probably because of the effect of the vibrations on the displacement of the deformed material.

## References


1. Hamadache H, Laouar L, Zeghib NE, Chaoui K (2006) Characteristics of Rb40 steel superficial layer under ball and roller burnishing. J Mater Process Tech 180:130–136
2. Luca L (2002) Investigation into the use of ball burnishing of hardened steel components as a finishing process. PhD Dissertation, University of Toledo, USA
3. Nemat M, Lyons AC (2000) An investigation of the surface topography of ball burnished mild steel and aluminum. Int J Adv Manuf Tech 16:460–473
4. Loh NH (1998) Effects of ball burnishing parameters on surface finish. a literature survey and discussion. Precis Eng 10:215–220
5. Prevey PS, Ravindranath RA, Shepard M, Gabb T (2003) Case studies of fatigue life improvement using low plasticity burnishing in gas turbine engine applications proceedings of ASME turbo expo. Atlanta, USA
6. Hassan AM, Sulieman ZS (1999) Improvement in the wear resistance of brass components by the ball burnishing process. J Mater Process Tech 96:73–80

7. Altenberger I, Nalla RK, Sano Y, Wagner L, Ritchie RO (2012) On the effect of deep-rolling and laser-peening on the stress-controlled low-and high-cycle fatigue behavior of Ti–6Al–4V at elevated temperatures up to 550 C. Int J Fatigue 44:292–302
8. Nalla RK, Altenberger I, Noster U, Liu GY, Scholtes B, Ritchie RO (2003) On the influence of mechanical surface treatments - deep rolling and laser shock peening- on the fatigue behavior of Ti–6Al–4V at ambient and elevated temperatures. Mat Sci Eng A-Struct 355(1):216–230
9. Shiou FJ, Chen CH (2003) Freeform surface finish of plastic injection mould by using ball burnishing process. J Mater Process Tech 140:248–254
10. Travieso-Rodriguez JA, Gonzalez-Rojas HA, Casado-Lopez R (2013) Herramienta con bola a baja presion, aplicable para bruñido de superficies. Spanish patent reference: P201130331. Boletin Oficial de la Propiedad Intelectual BOPI 21(11)
11. Lopez de la Calle LN, Rodriguez A, Lamikiz A, Celaya A, Alberdi R (2011) Five-Axis Machining and burnishing of complex parts for the improvement of surface roughness. Mater Manuf Process 26(8):997–1003
12. Hassan AM, Maqableh AM (2000) The effects of initial burnishing parameters on non-ferrous components. J Mater Process Tech 102:115–121
13. Yen YC, Altan T (2004) Finite element modelling of ball burnishing prediction of surface deformation and residual stress. ERC Report No. HPM/ERC/NSM-04-R-04, Ohio State University
14. Lopez de la calle LN, Lamikiz A, Sanchez JA, Arana JL (2007) The effect of ball burnishing on heat-treated steel and Inconel 718 milled surfaces. Int J Adv Manuf Tech 32(9–10):958–968
15. Gao XL (2003) Strain gradient plasticity solution for an internally pressurized thick-walled spherical shell of an elastic-plastic material. Mech Res Commun 30:411–420
16. Gao XL, Jing XN, Subhash G (2006) Two new expanding cavity models for indentation deformation of elastic strain-hardening materials. Int J Solids Struct 43:2193–2208
17. Sequera A, Fu CH, Guo YB, Wei XT (2014) Surface integrity of inconel 718 by ball burnishing. J Mater Eng Perform 23(9):3347–3353
18. Qu S, Huang Y, Pharr GM, Hwang KC (2005) The indentation size effect in the spherical indentation of iridium: a study via the conventional theory of mechanism-based gradient plasticity. Int J Plasticity 22:1265–1286
19. Nix WD, Gao H (1998) Indentation size effects in crystalline materials: a law for strain gradient plasticity. J Mech Phys Solids 46:411–425
20. Hernot X, Bartier O, Bekouche Y, El Abdi R, Mauvoisin G (2006) Influence of penetration depth and mechanical properties on contact radius determination for spherical indentation. Int J Solids Struct 43:4136–4153
21. Gomez-Gras G, Travieso-Rodriguez JA, Gonzalez-Rojas HA, Napoles-Alberro A, Carrillo F, Dessein G (2015a) Study of a ball burnishing vibration-assisted process. P I Mech Eng B-J Mec 229(1):172–177
22. Gomez-Gras G, Travieso-Rodriguez JA, Gonzalez-Rojas HA, Napoles-Alberro AE (2012) Influence of peak height prior to milling the resulting surface roughness of the ball burnishing process on convex and concave pieces of aluminum. In: Proceedings of the third international conference on surface metrology (ICSM3), Annecy, France, pp 26–34
23. Travieso-Rodriguez JA, Dessein G, Gonzalez-Rojas HA (2011) Improving the surface finish of concave and convex surfaces using a ball burnishing process. Mater Manuf Process 26(12):1494–1502
24. Travieso-Rodriguez JA, Gomez-Gras G, Dessein G, Carrillo F, Alexis J, Jorba-Peiro J, Aubazac N (2015b) Effects of a ball-burnishing process assisted by vibrations in G10380 steel specimens. Int J Adv Manuf Tech. doi:10.1007/s00170-015-7255-3
25. Travieso-Rodriguez JA, Gomez-Gras G, Jorba-Peiro J, Carrillo F, Dessein G, Alexis j, Gonzalez-Rojas H (2015b) Experimental study on the mechanical effects of the vibration-assisted ball burnishing process. Mater Manuf Process. doi:10.1080/10426914.2015.1019114
26. Gomez-Gras G (2015a) Estudio del proceso de bruñido con bola asistido por una vibracin. PhD dissertation Universitat Politcnica de Catalunya, Barcelona, Spain